Periodic forcing of a model sensory neuron

Carlo R. Laing*
Institute of Information and Mathematical Sciences, Massey University, Auckland, New Zealand

André Longtin
Department of Physics, University of Ottawa, Ottawa, Ontario, Canada K1N 8 P5

(Received 8 January 2003; published 27 May 2003)

We study the effects of sinusoidally modulating the current injected into a model sensory neuron from the weakly electric fish *Apteronotus leptorhynchus*. This neuron's behavior is known to switch from quiescence to periodic firing to bursting as the injected current is increased. The bifurcation separating periodic from bursting behavior is a saddle-node bifurcation of periodic orbits, and it has been shown previously that there is ''type-I burst excitability'' associated with this bifurcation, similar to the usual excitability associated with the transition from quiescence to periodic firing. Here we show numerically that sinusoidal modulation of the dc current injected into the model neuron can switch it from periodic to burst firing, or vice versa, depending on the frequency of modulation and the distance to the burst excitability threshold. This is explained by mapping resonance tongues in parameter space. We also show that such a model neuron can undergo stochastic resonance near the transition from periodic to burst firing, as a result of the burst excitability, regardless of the location (soma or dendrite) of the signal and noise. The novelty is that the ''output event'' is now a burst rather than a single action potential, and the neuron returns to almost periodic firing between bursts, rather than to the vicinity of a fixed point. Since the neuron under study is a sensory neuron that must encode signals with varying temporal structure in the presence of considerable intrinsic noise, these aspects are of potential importance to electrosensory processing and also to other bursting neurons that have periodic input.

DOI: 10.1103/PhysRevE.67.051928 PACS number(s): 87.19.La, 05.45.−a, 05.40.−a

I. INTRODUCTION

Bursting, in which a cell periodically switches from a quasi-steady state to a rapidly spiking state and back again, is an important and common form of behavior [1–6]. Many of the cells that do show bursting are deep within a network of other cells [2], and it is difficult to determine the nature of their inputs. However, a particular bursting mechanism in a sensory neuron with a well-characterized input has recently been described [3,7]. This type of cell is a pyramidal cell in the electrosensory lateral line lobe (ELL) of the weakly electric fish, *Apteronotus leptorhynchus*. These fish continuously generate a weak electrical field known as the electric organ discharge (EOD). The field permeates the fish's environment, interacting with it, and is detectable by both the emitting fish and other nearby fish. The fish detect the field with electroreceptors on their skin, which then transmit information to the pyramidal cells. Thus, these pyramidal cells are very close to the start of the sensory pathway from the periphery to the brain of the fish.

The amplitude of the EOD is approximately sinusoidal and the frequency of a given fish is constant within the species range of 600–1200 Hz. The electroreceptors on a fish's skin can detect both the amplitude and phase of this quasisinusoidal signal. These properties of the signal will be modified by, e.g., a prey object, a rock, or another fish [8,9]. Also, a ''beat'' frequency occurs when two fish with different frequencies meet (the beat frequency is equal to the difference between the frequencies of the two fish). Thus, there are at least two approximately sinusoidal inputs that can be detected by the electroreceptors and passed to the pyramidal cells that we model. There has also been recent interest in stochastic biperiodic oscillations in paddlefish electroreceptors [10], and some of our results may be applicable to that situation.

A six-variable ODE model of a pyramidal cell from *A. leptorhynchus* (henceforth referred to as a ''ghostburster'') has recently been developed [7]. This model reproduced qualitatively, and to a large extent quantitatively, the behavior observed both in real pyramidal cells from the ELL [3] and in a many-variable morphologically realistic model [11]. Due to the small number of variables in the ghostburster model, we can easily investigate how it reacts to time-varying stimuli. A previous paper [12] investigated how the ghostburster reacts to transient stimuli; in it, the concept of ''type-I burst excitability'' was presented. Briefly, burst excitability is a generalization of ''normal'' excitability [1,5], but the ''event'' is a burst of action potentials rather than a single one, and the ''rest state'' that the system returns to after the event may be, for example, a periodic orbit, rather than an actual fixed point of the system (''quiescence''). With this knowledge of both the burst attractor and the excitable nature of the ghostburster system, we investigate the effects of sinusoidal input to the ghostburster model [7].

The response of nonlinear systems, particularly oscillators, to periodic forcing is a much studied problem, and the work here can be thought of as a generalization of the results for periodically forced oscillators [13–16] and periodically forced excitable systems [17,18]. A number of qualitatively different types of bursting behavior have been observed and analyzed [1,5,6], and it would be of interest to understand

*Electronic address: c.r.laing@massey.ac.nz

how these other systems respond to time-varying inputs. It is likely that this information would also help in understanding how coupled bursting systems behave, an area of recent interest [19]. Here we choose to study the ghostburster, as it is well characterized experimentally and has a clearly defined and relevant periodic input.

A two-variable model of the bursting pyramidal cell studied here was presented in Ref. [20], along with an analysis of its response to sinusoidal input currents. However, that model was a caricature of the cell and only reproduced the qualitative aspects of ghostbursting. The model studied here is quantitatively correct with respect to time scales and voltage wave forms, and agrees well with the behavior seen in experiments [3] and much more complicated models [11].

Noise is ubiquitous in neural systems, and can result from the probabilistic nature of the opening and closing of ion channels, or the stochastic nature of synaptic transmission, among other things [21]. The pyramidal cells under study here are known to be intrisically noisy when unstimulated [22]. The importance of the presence of noise in the nervous system of *A. leptorhynchus* is not clear, but we will look at the generic features of the response of the ghostburster model to both noise and noise combined with a periodic signal.

In Sec. II, we introduce the ghostburster and summarize its relevant features. Section III discusses the effects of sinusoidal inputs on the ghostburster model, and Sec. IV demonstrates the existence of stochastic resonance in the model. We conclude in Sec. V.

II. GHOSTBURSTER MODEL

We now give a brief summary of the burst mechanism investigated in Ref. [7]. The model equations are presented in the Appendix, and details of the large model they are derived from are in Ref. [11]. Both the soma and dendrite of the neuron were found to be capable of initiating action potentials, and a somatic action potential typically induced a corresponding dendritic action potential via active backpropagation down the dendritic tree. The dendritic action potentials have a longer half-width than the somatic, and the dendritic refractory period is thus longer than that of the somatic. Because of this difference, near the end of a dendritic action potential some current flows from the dendrite to the soma, causing a depolarizing afterpotential (DAP) to appear after the corresponding somatic action potential.

For small dc current injections to the soma, the cell fires periodically, with dendritic action potentials tracking the somatic ones. However, for larger current injections, the dendritic potassium inactivation gating variable (p_d, see the Appendix) cannot fully recover between action potentials, and this variable gradually decreases during the course of a number of action potentials, leading to a broadening of dendritic action potentials, an increase in the DAP size, and a slow increase in firing frequency. This continues until a somatic interspike interval (ISI) is smaller than the refractory period of the dendrite, and the dendrite no longer fires an action potential in response to a somatic one. This results in a long ISI, during which the dendritic potassium inactivation variable recovers, and another burst commences. Thus, a burst consists of a number of action potentials whose ISIs monotonically decrease, separated by a long ISI. See Fig. 1 for an example.

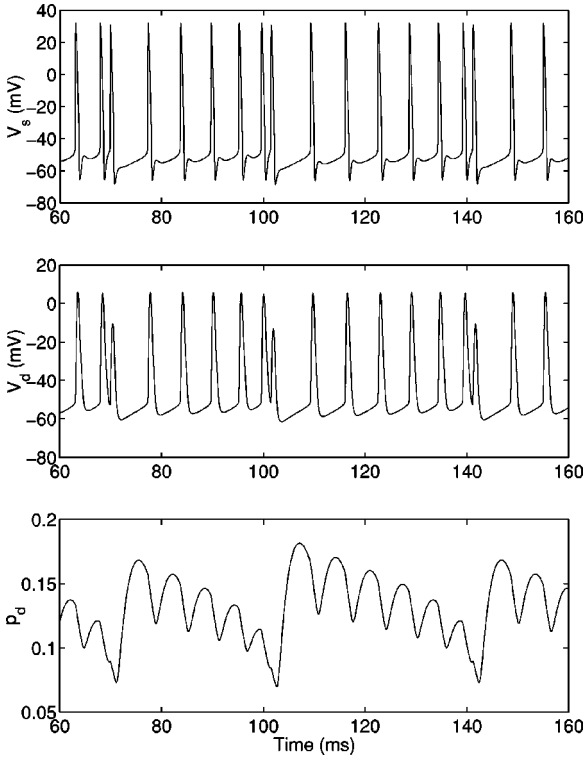

FIG. 1. An example of ''ghostbursting'' for the model presented in Ref. [7]. The equations are given in the Appendix. Top, somatic voltage; middle, dendritic voltage; bottom, dendritic potassium inactivation (p_d). Each burst terminates with a short ISI (a doublet) that is immediately followed by a long one. This occurs at $t \approx 70$, 100, and 140 ms. DAPs are visible after most somatic action potentials. Note the reduced height of the dendritic action potential at the end of each burst. The injected current is $I = 9.5$.

From the above description, we see that if the magnitude of a dc current injected to a pyramidal cell is slowly increased, the cell changes from quiescent (not firing action potentials) to periodic firing of action potentials to bursting. This is shown in Fig. 2. This ordering is in contrast with many other burst mechanisms, where the sequence is often quiescent $\rightarrow$ bursting $\rightarrow$ periodic firing, as the injected current is increased [5,23,24].

The threshold between periodic and bursting behavior is very important if these neurons are thought of as being involved in feature detection (i.e., encoding up- or downstrokes of the electric field amplitude [25,26]), since the information from other cells will likely be manifested as a change in input current to a pyramidal cell, which may then cause a change from periodic firing to bursting or vice versa. Lisman [4] has also proposed that bursts rather than action potentials could be the fundamental unit of information, as a burst combined with synaptic facilitation may be far more reliable than a single action potential, for example.

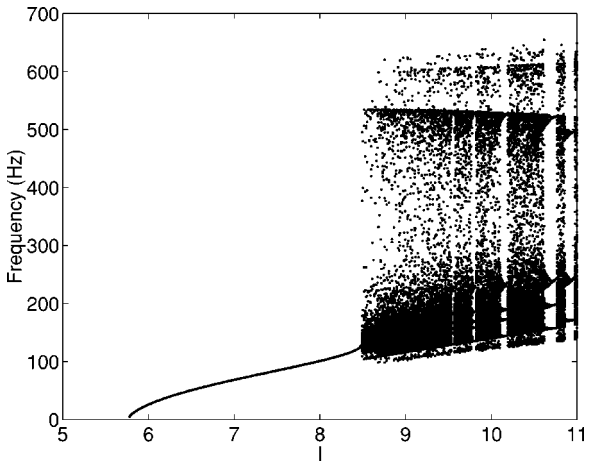

FIG. 2. A plot of instantaneous firing frequency (reciprocal of each interspike interval) as a function of input current to the soma, I, for the ODE model presented in Ref. [7]. The cell moves from quiescence to periodic firing at $I \approx 5.7$, and from periodic firing to bursting at $I \approx 8.5$. In Ref. [7] it was determined that the two corresponding bifurcations are a saddle-node bifurcation on a circle, and a saddle-node bifurcation of periodic orbits, respectively. For each value of I, all ISIs within a 500 ms window after transients had died down were used. The equations are given in the Appendix.

III. SINUSOIDAL INPUT

We now investigate the effects of sinusoidally modulating the somatic input current to the ghostburster, replacing I in Eq. (A1) with $I_b + I_{mod}\sin(2\pi ft)$, where I_b is the constant component of the current, I_{mod} is the amplitude of the modulation, and f is the frequency of modulation. We are mainly interested in whether varying I_{mod} and f can cause the model to switch from periodic firing to bursting or vice versa.

Figure 3 shows the effects of this form of modulation as a function of both I_b and f for the ghostburster (A1)–(A6). The color indicates the reciprocal of the minimum ISI measured during a 250 ms period. The darkest colors indicate that the cell is bursting, as we are detecting the high-frequency ''doublet'' that signifies the end of a burst (see Fig. 1). A number of features are apparent: from Fig. 2 we see that without modulation, the periodic to burst threshold is at $I_b \approx 8.5$, so modulation can push the apparent threshold to either higher I_b values (e.g., for f near 120 Hz) or lower I_b values (e.g., for $f < 50$ Hz).

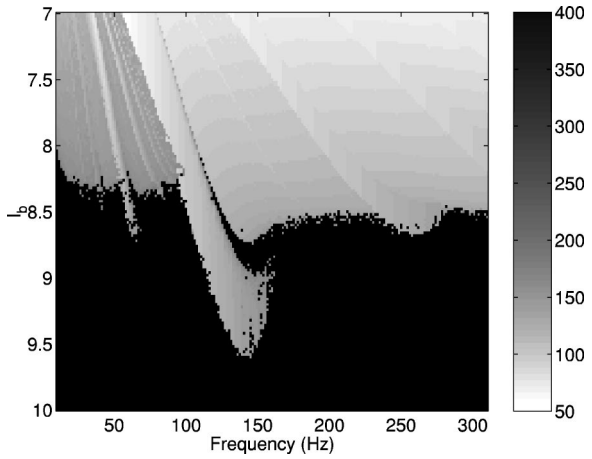

FIG. 3. Modification of burst threshold in model (A1)–(A6) by sinusoidal forcing. The input current is $I_b + 1.5\sin(2\pi ft)$, where f is the frequency of forcing (plotted horizontally). The color indicates the maximum instantaneous firing frequency in Hz (reciprocal of the instantaneous ISI) during 250 ms. In the absence of forcing, the periodic or bursting transition occurs at $I_b \approx 8.5$ (see Fig. 2).

Much of Fig. 3 can be understood by remembering that below burst threshold, the cell fires periodically, i.e., it is an oscillator. Entrainment of oscillators to an external forcing frequency has been well studied [14,15,13,16]. It is known that regions of parameter space can exist in which the frequencies of the driving and driven oscillators have a simple ratio, e.g., 2:3. These regions are known as ''Arnold tongues,'' and are labeled by the ratio of the driving to driven frequencies, in its simplest form. The most prominent in Fig. 3 is the 1:1 tongue, stretching from $(f, I_b) \approx (70,7)$ to $\approx (150,9.5)$. (The tongue stretches down and to the right because as I_b is increased, the frequency of the oscillator increases, see Fig. 2.) The 2:1 tongue can also be seen, terminating at $(f, I_b) \approx (260,8.6)$. In this region, the neuron fires one action potential on every second forcing cycle, i.e., the ratio of driving to driven frequencies is 2:1. Further tongues are seen in the top left corner of Fig. 3.

The observation that some Arnold tongues cross the periodic to burst threshold in the unforced system ($I_b = 8.5$) is similar to the results of Yoshino *et al.* [18] who studied the Arnold tongue structures in a periodically forced system that, when the amplitude of forcing was zero, could be either excitable from a quiescent state or oscillating periodically. They found that as the parameter controlling the excitable $\rightarrow$ oscillatory transition was varied across the boundary for a fixed amplitude of periodic forcing, the Arnold tongue structure was continuous. We also see this. In Fig. 3, if I_b is increased through 8.5 for $f = 110$ Hz, the system remains in the 1:1 locked state, firing periodically, even though the unforced dynamics ($I_{mod} = 0$) have changed from periodic firing to bursting. In other words, periodic stimulation at 100 Hz postpones the onset of bursting.

Figure 4 shows the Arnold tongues in the more usual amplitude/frequency of forcing space, and demonstrates how the bursting behavior modifies the tongues. In Fig. 4, top ($I_b = 8$), the 1:1 tongue is seen starting at $(f, I_{mod}) \approx (100,0)$ and the 2:1 tongue (where there is one action potential for every two forcing cycles) starts at $(f, I_{mod}) \approx (200,0)$. Thinner tongues are seen, as well as bursting for f less than about 80 Hz. Thus, bursting is induced for sufficiently slow and strong forcing. This can be understood as resulting from the modulation being so slow that it is effectively constant over time intervals on the order of the duration of a burst. Thus, if the modulation amplitude is strong enough, at least one burst will be induced during part of each forcing cycle. Figure 4, bottom, has $I_b = 8.7$, so that for $I_{mod} = 0$, the cell is bursting. Despite this, sufficiently strong forcing at sufficiently high frequencies can suppress bursting. The tongue with edges at $(f, I_{mod}) \approx (95,3)$ and $(120,3)$ is the 1:1 tongue.

For some of the parameter values shown in Figs. 3 and 4,

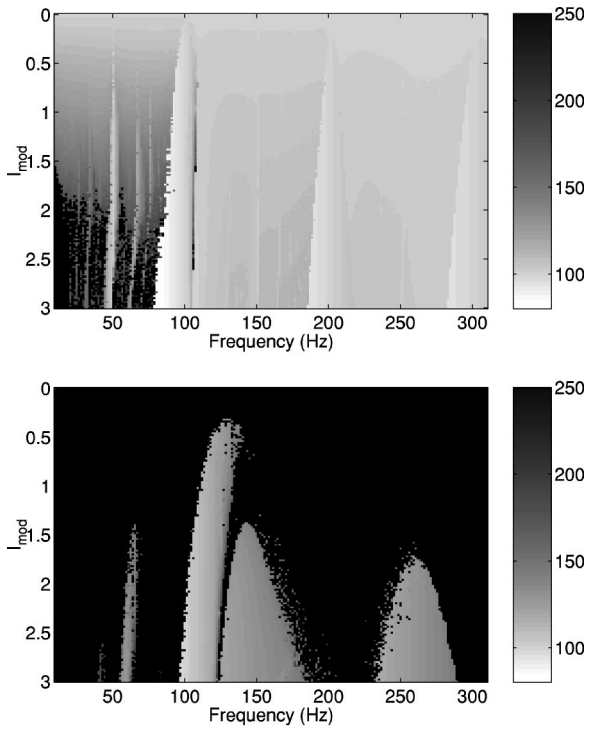

FIG. 4. Arnold tongues in amplitude/frequency of forcing space for Eqs. (A1)–(A6). The input current is $I_b+I_{mod}\sin(2\pi ft)$. Top, $I_b=8$; when $I_{mod}=0$ the neuron is not bursting. Bottom, $I_b=8.7$; when $I_{mod}=0$ the neuron is bursting. The color indicates the maximum instantaneous firing frequency in Hz (reciprocal of the minimum ISI).

system (A1)–(A6) with I being periodically modulated is bistable. The two attractors are bursting behavior and periodic firing that is frequency locked to the forcing. Only one maximum frequency was calculated at each of the points in Figs. 3 and 4, and the bistability appears as the ''speckles'' of light within dark regions and dark within light regions. This bistability was also found when the reduced model presented in Ref. [20] was periodically forced, in the vicinity of the 1:1 locked orbit. There it was found to arise from a subcritical Hopf bifurcation of that orbit.

From Fig. 3, we see that the boundary between periodic and bursting behavior is deformed when $I_{mod}\neq 0$. It is deformed to lower I_b values for some frequencies and to higher I_b values for other frequencies. This suggests that if I_{mod} is suddenly switched from zero to a nonzero value, the neuron could be induced to switch from periodic firing to bursting, or vice versa, depending on the value of I_b and the forcing frequency. Examples of both of these types of behaviors are shown in Figs. 5 and 6, where a sinusoidal modulation of I is applied for a few hundred milliseconds. In Fig. 5, the bursting is suppressed almost immediately and the neuron is induced to fire at the same frequency as the forcing. In Fig. 6, a high-frequency doublet occurs within 100 ms of the onset of forcing. We now examine the effects of including noise in the dynamics of the ghostburster.

IV. STOCHASTIC RESONANCE

Stochastic resonance is a well-known phenomenon in nonlinear dynamical systems [27,28]. Put simply, the addition of a small amount of noise to a system receiving a subthreshold signal may make the signal observable. When no noise is added, the signal is, by definition, unobservable, and if large amounts of noise are added, the signal is swamped by the noise. Thus, if the signal to noise ratio for a periodic signal is plotted as a function of noise level, it will have a maximum at some intermediate intensity of noise. This maximum may have some functional significance for an ''observer'' of the system.

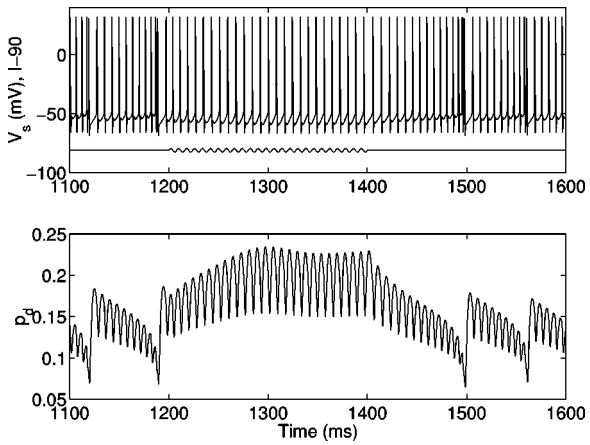

FIG. 5. A transient sinusoidal modulation of the input current switches system (A1)–(A6) from bursting to periodic firing. Parameters are $I_b=9$, I_{mod} is 1.5 for $1200<t<1400$, and the forcing frequency is 125 Hz. Top, V_s and $I-90$; bottom, p_d. Note that the neuron is induced to fire at the same frequency as the forcing (1:1 locking).

As seen in Fig. 2, the ghostburster (A1)–(A6) has two current thresholds, i.e., there are two values of I such that, if I is transiently increased above these values, there is a qualitative change in the behavior of the system. The first threshold, at $I\approx 5.6$ involves a saddle node on a circle bifurcation, i.e., excitable dynamics between a fixed point and periodic firing, so the system is capable of exhibiting stochastic reso-

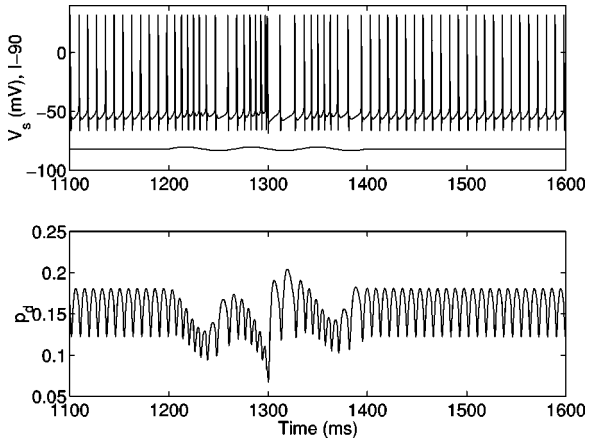

FIG. 6. A transient sinusoidal input switches system (A1)–(A6) from periodic to burst firing. Parameters are $I_b=8.3$, I_{mod} is 1.5 for $1200<t<1400$, and the forcing frequency is 15 Hz. Top, V_s and $I-90$; bottom, p_d. One burst is induced, which terminates at $t=1300$ ms.

nance near this threshold [28]. We now show that the ghostburster can also show stochastic resonance near the periodic $\rightarrow$ burst threshold that occurs for larger bias current I, provided that bursts are used to form the output signal, rather than individual action potentials.

We include the effects of noise by adding a Gaussian white noise current term $\eta(t)$ to the first (current balance) equation in (A1)–(A6), where $\langle \eta(t) \rangle = 0$ and $\langle \eta(t)\eta(s) \rangle = 2D\delta(t-s)$, so that D is a measure of the noise intensity. This term is meant to mimic the fluctuations in ion channel conductances, the effects of the probabilistic nature of synaptic transmission, and the other sources of randomness that occur in neural systems [21]. The signal we use is a $10/(2\pi)$ Hz sinusoidal modulation of the current with $I_b = 8.4$ and $I_{mod} = 0.15$, i.e., we have $I = 8.4 + 0.15\sin(10t)$. This is quite a slow and weak modulation compared with the frequencies involved in the Arnold tongues (see Figs 3 and 4). Note that when $D = 0$ and I is as above the model neuron does not burst; instead, the instantaneous firing rate is sinusoidally modulated by the current.

In contrast with normal excitability, where the ''event'' is an action potential, the event in burst excitability is a burst [12], which is easily detected for model (A1)–(A6) by monitoring ISIs, since a burst always terminates in a high-frequency doublet. (In Ref. [12], the response of the ghostburster to transient, steplike inputs was examined; here we examine the response to continuous sinusoidal modulations of the input current.) In practice, the end of a burst could be detected by a facilitating synapse [29] that would preferentially transmit the last few action potentials that occur in quick succession [4]. To quantify stochastic resonance in the ghostburster, we detect all ISIs less than 4 ms and record the time t_i of the second action potential of the ISI. In a similar way to that done in [20] for a ''toy'' model of the ghostburster, we form an output signal consisting of δ functions at times t_i:

$$f(t) = \sum_i \delta(t - t_i), \tag{1}$$

where the sum is over all such times during a finite-time simulation. Passing $f(t)$ through a Hanning window defined over the length of the simulation, T, and taking the Fourier transform, we have

$$F(\omega) = \frac{1}{2} \sum_i e^{i\omega t_i} \left[1 - \cos\left(\frac{2\pi t_i}{T} \right) \right] \tag{2}$$

and the power spectrum of $f(t)$ is $|F(\omega)|^2$.

Typical spectra for three different noise intensities are shown in Fig. 7. It is clear that the power at the driving frequency, $f = 10/(2\pi)$ Hz, increases and then decreases as D is increased, and that the background noise intensity monotonically increases as D is increased.

The signal to noise ratio as a function of D is shown in Fig. 8. The signal strength was defined to be the power density at the forcing frequency [$f = 10/(2\pi)$ Hz] and the noise strength was defined to be the average of the power in the two bands $7 < 2\pi f < 9$ and $11 < 2\pi f < 13$. (The spectra are essentially flat with no obvious peaks for $5 < 2\pi f < 9.9$ and $10.1 < 2\pi f < 15$, not shown.) Five simulations of 200 s each were used to calculate the values shown in Fig. 8. This clearly confirms the results suggested by Fig. 7 and shows that system (A1)–(A6) can demonstrate stochastic resonance near the periodic or bursting boundary, provided that the ''output signal'' is taken to be a burst. If, instead, all action potentials are used to form a signal [i.e., the t_i in Eq. (1) are the occurrence times of every action potential], the signal to noise ratio decreases monotonically as noise intensity is increased (not shown).

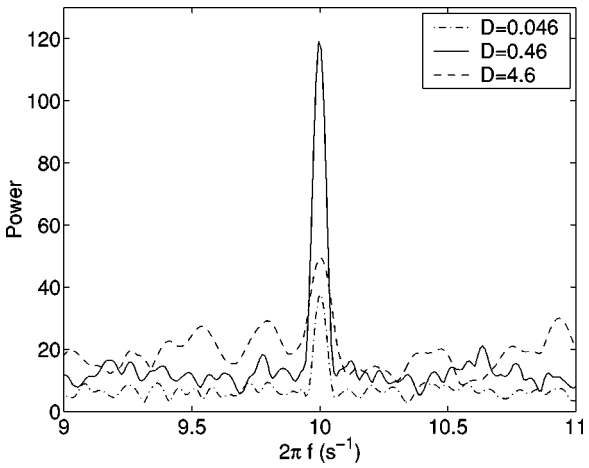

FIG. 7. Power spectra from Eq. (2) for three different values of D for the ghostburster, Eqs. (A1)–(A6). The driving frequency was $f = 10/(2\pi)$ Hz. Five independent realizations of 200 s each have been averaged to obtain each spectrum.

Thus, we have shown that if a burst is regarded as the fundamental unit of information [4], as opposed to an action potential, the model of a sensory neuron studied here is capable of undergoing stochastic resonance. This complements the results presented in Ref. [12], where it was shown that a

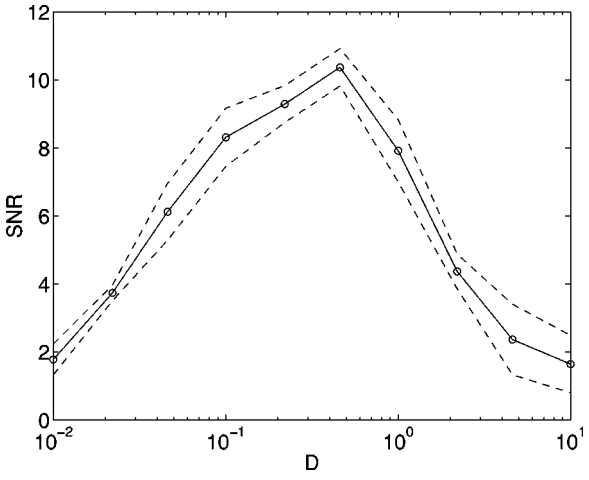

FIG. 8. Signal to noise ratio (defined in the text) as a function of noise intensity D for the ghostburster, Eqs. (A1)–(A6). The dashed lines indicate ± 1 standard deviation. Five independent realizations of 200 s each for each value of D chosen were used to calculate the SNR.

transient increase in synaptic input to such a model neuron could be robustly signaled by the production of a burst.

The results presented here are for an input signal and noise added to the soma only. Biophysically, however, inputs to a neuron are thought of as coming via the dendrites. Also, it is not clear what relative contribution do the soma and dendrite make to the overall level of noise in a neuron. Thus, it would be interesting to see whether stochastic resonance occurs in the ghostburster when the signal is injected to the dendrite and noise appears in either the soma or dendrite. We investigated these possibilities and found that stochastic resonance does occur, regardless of the location (soma or dendrite) of the injected signal and the noise term (not shown).

We also investigated the behavior of the ghostburster in the vicinity of the periodic to burst threshold with noise applied to the soma but no periodic input signal. In analogy with other excitable systems, if the input current was held just below the threshold and noise was added, we might expect to see coherence resonance [30] as the noise intensity was increased, again using a burst as the output ''signal.'' The bursts would be irregular at low noise intensity, more regular at medium intensity, and irregular again at high noise intensity. However, we did not observe this. One possible explanation is that, even in the noise-free system, bursts do not have a well-defined duration (see Fig. 1), and thus there is not a characteristic time scale that can be ''uncovered'' by the noise. In fact, the bursting is chaotic [7], which is thought to invalidate general descriptions of coherence resonance [30]. Another contributing factor may be that after one burst (in the noise-free case), the system does not necessarily have to return directly to the periodic state; it may instead undergo one or more further bursts before returning to the periodic state, as was demonstrated in Ref. [12].

Another possibility would be to observe autonomous stochastic resonance [31,32], where the height of a particular peak in the output spectrum reaches a maximum at some intermediate noise intensity. However, we did not observe this either, probably as a result of the factors mentioned above.

V. CONCLUSION

We have studied the response of a particular model neuron to sinusoidal modulations of its input current. In the absence of modulation, this particular neuron has a well-defined current threshold between periodic and burst firing. Modulations move this threshold, either increasing or decreasing it, depending on the frequency of modulation.

Because of the bifurcation involved in the threshold and the flow of orbits in phase space, the model neuron shows type-I burst excitability at this boundary [12]. This implies that if a subthreshold modulation of the current is applied, together with some type of noise, the system should show stochastic resonance. We demonstrated that it does, once it is recognized that the output signal involves a burst rather than an individual action potential.

The particular neuron modeled here is a sensory neuron in the weakly electric fish *A. leptorhynchus*, and is close to the periphery of the fish. There are at least two sources of periodic input to these cells—the fish's own electric organ discharge, and the beat frequency created when two fish are close to one another. Thus, it is of interest to understand how these cells react to such inputs.

More generally, there are many types of bursting neurons; these are often classified in terms of the bifurcations involved in the transition between quiescence and periodic firing and the transition between periodic firing and quiescence [1]. They are found in many different parts of the nervous systems of many different species [2]. The response of oscillators and excitable systems to periodic forcing has been much studied [14–16,13,18,17], and a natural generalization of this is the study of the response of bursting systems to periodic forcing. The study presented here, although by no means complete and only involving one model, is a first step in that direction.

ACKNOWLEDGMENTS

I thank Brent Doiron and Len Maler for useful conversations regarding this work. This work was partially funded through OPREA and the Natural Sciences and Engineering Research Council of Canada.

APPENDIX: GHOSTBURSTER EQUATIONS

We present here the governing differential equations for the model neuron studied in this paper. The model consists of two isopotential compartments, representing the soma and dendrite of the neuron, diffusively coupled through voltage. The equations, previously presented in [7], are

$$C\frac{dV_s}{dt} = I - g_{Na,s}[m_{\infty,s}(V_s)]^2(h_0 - n_s)(V_s - V_{Na}) - g_{dr,s}n_s^2(V_s - V_K) - g_L(V_s - V_L) - \frac{g_c}{\kappa}(V_s - V_d), \tag{A1}$$

$$\frac{dn_s}{dt} = \frac{n_{\infty,s}(V_s) - n_s}{0.39}, \tag{A2}$$

$$C\frac{dV_d}{dt} = -g_{Na,d}[m_{\infty,d}(V_d)]^2 h_d(V_d - V_{Na}) - g_{dr,d}n_d^2 p_d(V_d - V_K) - g_L(V_d - V_L) - \frac{g_c}{1-\kappa}(V_d - V_s), \tag{A3}$$

$$\frac{dh_d}{dt} = h_{\infty,d}(V_d) - h_d, \tag{A4}$$

$$\frac{dn_d}{dt} = \frac{n_{\infty,d}(V_d) - n_d}{0.9}, \tag{A5}$$

$$\frac{dp_d}{dt} = \frac{p_{\infty,d}(V_d) - p_d}{5}. \tag{A6}$$

Time is measured in milliseconds and voltages are measured in millivolts. Subscripts *s* and *d* refer to somatic and dendritic variables, respectively. *m* and *h* are activation and inactivation of Na^+, respectively, and *n* and *p* are activation and inactivation of K^+, respectively. Parameter values are $C=1\,\mu\mathrm{F/cm}^2$, $g_{Na,s}=55$, $h_0=1$, $V_{Na}=40$, $g_{dr,s}=20$, $V_K=-88.5$, $g_L=0.18$, $V_L=-70$, $g_c=0.4$, $\kappa=0.4$, $g_{Na,d}=5$, $g_{dr,d}=15$. Conductances are measured in $\mathrm{mS/cm}^2$, I is the input current, g_c is the coupling conductance, and κ is the ratio of the somatic area to the total area of the cell. Other functions are $m_{\infty,s}(V)=1/\{1+\exp[-(V+40)/3]\}$, $n_{\infty,s}(V)=1/\{1+\exp[-(V+40)/3]\}$, $m_{\infty,d}(V)=1/\{1+\exp[-(V+40)/5]\}$, $h_{\infty,d}(V)=1/\{1+\exp[(V+52)/5]\}$, $n_{\infty,d}(V)=1/\{1+\exp[-(V+40)/5]\}$, $p_{\infty,d}(V)=1/\{1+\exp[(V+65)/6]\}$. For details and derivation of these equations, see Refs. [7,11].

[1] E.M. Izhikevich, Int. J. Bifurcation Chaos Appl. Sci. Eng. **10**, 1171 (2000).

[2] J. Keener and J. Sneyd, *Mathematical Physiology* (Springer-Verlag, New York, 1998).

[3] N. Lemon and R. Turner, J. Neurophysiol. **84**, 1519 (2000).

[4] J.E. Lisman, Trends Neurosci. **20**, 38 (1997).

[5] J. Rinzel and G.B. Ermentrout, in *Methods in Neuronal Modeling: From Ions to Networks*, edited by C. Koch and I. Segev (MIT, Cambridge, MA, 1998).

[6] G. de Vreis, J. Nonlinear Sci. **8**, 281 (1998).

[7] B. Doiron, C.R. Laing, A. Longtin, and L. Maler, J. Comput. Neurosci. **12**, 5 (2002).

[8] M.E. Nelson, Z. Xu, and J.R. Payne, J. Comp. Physiol., A **181**, 532 (1997).

[9] M.J. Chacron, A. Longtin, and L. Maler, J. Neurosci. **21**, 5328 (2001).

[10] A. Neiman and D.F. Russel, Phys. Rev. Lett. **86**, 3443 (2001).

[11] B. Doiron, A. Longtin, R.W. Turner, and L. Maler, J. Neurophysiol. **86**, 1523 (2001).

[12] C.R. Laing, B. Doiron, A. Longtin, L. Noonan, R.W. Turner, and L. Maler, J. Comput. Neurosci. **14**, 329 (2003).

[13] S. Coombes and P.C. Bressloff, Phys. Rev. E **60**, 2086 (1999).

[14] L. Glass and M.C. Mackey, *From Clocks to Chaos: The Rhythms of Life* (Princeton University Press, Princeton, NJ, 1988).

[15] L. Glass, Chaos **1**, 13 (1991).

[16] W.N. Vance and J. Ross, Chaos **1**, 445 (1991).

[17] J.C. Alexander, E.J. Doedel, and H.G. Othmer, SIAM (Soc. Ind. Appl. Math.) J. Appl. Math. **50**, 1373 (1990).

[18] K. Yoshino, T. Nomura, K. Pakdaman, and S. Sato, Phys. Rev. E **59**, 956 (1999).

[19] E.M. Izhikevich, SIAM Rev. **43**, 315 (2001).

[20] C.R. Laing and A. Longtin, Bull. Math. Biol. **64**, 829 (2002).

[21] C. Koch, *Biophysics of Computation: Information Processing in Single Neurons* (Oxford University Press, Oxford, 1999).

[22] J. Bastian and J. Nguyenkim, J. Neurophysiol. **85**, 10 (2001).

[23] P.F. Pinsky and J. Rinzel, J. Comput. Neurosci. **1**, 39 (1994).

[24] D. Terman, J. Nonlinear Sci. **2**, 135 (1992).

[25] F. Gabbiani and W. Metzner, J. Exp. Biol. **202**, 1267 (1999).

[26] F. Gabbiani, W. Metzner, R. Wessel, and C. Koch, Nature (London) **384**, 564 (1996).

[27] L. Gammaitoni, P. Hänggi, P. Jung, and F. Marchesoni, Rev. Mod. Phys. **70**, 223 (1998).

[28] K. Wiesenfeld and F. Jaramillo, Chaos **8**, 539 (1998).

[29] R.S. Zucker and W.G. Regehr, Annu. Rev. Physiol. **64**, 355 (2002).

[30] A.S. Pikovsky and J. Kurths, Phys. Rev. Lett. **78**, 775 (1997).

[31] H. Gang, T. Ditzinger, C.Z. Ning, and H. Haken, Phys. Rev. Lett. **71**, 807 (1993).

[32] A. Longtin, Phys. Rev. E **55**, 868 (1997).